ARTICLE
Journal of Cellular Biochemistry 112:341–353 (2011)

Journal of Cellular Biochemistry

Urotensin II Receptor Predicts the Clinical Outcome of Prostate Cancer Patients and Is Involved in the Regulation of Motility of Prostate Adenocarcinoma Cells

Paolo Grieco,[1] Renato Franco,[2] Giuseppina Bozzuto,[3] Laura Toccacieli,[3] Alessandro Sgambato,[5] Monica Marra,[5] Silvia Zappavigna,[5] Mario Migaldi,[6] Giulio Rossi,[6] Stefano Striano,[7] Luigi Marra,[7] Luigi Gallo,[7] Achille Cittadini,[4] Gerardo Botti,[2] Ettore Novellino,[3] Agnese Molinari,[3] Alfredo Budillon,[5] and Michele Caraglia[5]*

[1] *Department of Pharmaceutical and Toxicological Chemistry, University of Naples Federico II, Naples, Italy*

[2] *Pathology Unit, National Institute of Tumours, Fondazione ''G. Pascale'', Naples, Italy*

[3] *Department of Technology and Health, Italian National Institute of Health, Rome, Italy*

[4] *Institute of General Pathology, ''Giovanni XXIII'' Cancer Research Center, Catholic University of Sacred Heart, Rome, Italy*

[5] *Experimental Pharmacology Unit, National Institute of Tumours, Fondazione ''G. Pascale'', Naples, Italy*

[6] *Dipartimento di Laboratori, Anatomia Patologica e Medicina Legale, University of Modena and Reggio Emilia, Modena, Italy*

[7] *Uro-Gynecological Department, National Institute of Tumours, Fondazione ''G. Pascale'', Naples, Italy*

ABSTRACT

Urotensin II (UT-II) is a potent vasoconstrictor peptide and its receptor (UTR) was correlated with human cortico-adrenal carcinoma proliferation. In this study, we have evaluated the correlation between UTR expression and prognosis of human prostate adenocarcinoma and the involvement of this receptor in the regulation of biological properties on both in vivo and in vitro models. UTR mRNA and protein, evaluated by real-time PCR and Western blotting, respectively, were expressed at high levels only in androgen-dependent LNCaP cells. In order to investigate UTR changes occurring in human prostate tumorigenesis, we have also evaluated the expression of UTR in vivo in 195 human prostate tissue samples. UTR was always expressed at low intensity in hyperplastic tissues and at high intensity in well-differentiated carcinomas (Gleason 2–3). Moreover, we have evaluated the effects of an antagonist of UTR, urantide on migration and invasion of LNCaP cells. Urantide induced a dose-dependent decrease of motility and invasion of LNCaP cells whose characteristic ameboid movement seems to be advantageous for their malignancy. These effects were paralleled by down-regulating the autophosphorylation of focal adhesion kinase and the integrin surface expression on LNCaP cells. The effects on cell motility and invasion were likely due to the inhibition of RhoA activity induced by both urantide and shRNA UTR. These data suggest that UTR can be considered a prognostic marker in human prostate adenocarcinoma patients. J. Cell. Biochem. 112: 341–353, 2011.

KEY WORDS: UROTENSIN II RECEPTOR; PROSTATE CANCER; PROGNOSTIC MARKER

Urotensin II (UT-II) was isolated from the urophysis of teleost fishes. Human UT-II is an 11 amino acid peptide that retains the cyclic portion typical of fish UT-II. It is the endogenous ligand of a G-protein-coupled receptor (GPCR) which was isolated from a human genomic library and displays high sequence similarity to GPR14, an orphan receptor currently referred to as the urotensin receptor (UTR) [Carotenuto et al., 2004].

The authors declare no personal or financial conflict of interest.

Paolo Grieco and Renato Franco equally contributed to this study.

Grant sponsor: Italian Ministry of Health FSN 2007-Progetto Strategico Oncologia.

Monica Marra's present address is Department of Biochemistry and Biophysics, Second University of Naples, Via Costantinopoli, 16 80138 Naples, Italy.

*Correspondence to: Prof. Michele Caraglia, Department of Biochemistry and Biophysics, Second University of Naples, Via Costantinopoli, 16 80138 Naples, Italy. E-mail: michele.caraglia@unina2.it

Received 13 July 2010; Accepted 19 October 2010 • DOI 10.1002/jcb.22933 • © 2010 Wiley-Liss, Inc.

Published online 15 November 2010 in Wiley Online Library (wileyonlinelibrary.com).

The human UTR has been found predominantly in the heart and arterial vessels, whereas UT-II like immunoreactivity can be detected in the macrophage and smooth muscle-rich region of human coronary atherosclerotic plaques [Ames et al., 1999]. Structure–activity relationship studies revealed that the cyclic portion (Cys5–Cys10) of the peptide is crucial for biological activity and the Trp7-Lys8-Tyr9 sequence has been shown to be the most important for h-UTR activation [Carotenuto et al., 2004; Lavecchia et al., 2005].

Recently, a UT-II analog ([Pen5,DTrp7,Orn8]urotensin-II(4–11)) named urantide, has been proposed as a selective and potent UTR antagonist, being about 50- to 100-fold more potent than any other known compound in the rat isolated aorta [Patacchini et al., 2003].

However, urantide mimicked the effects of UT-II on $[Ca2+]_i$ release in CHO cells transfected with human UT (CHOhUT cells) thus acting as a UT receptor agonist [Camarda et al., 2004]. In this assay, the peptide displayed a potency value lower than that one of UT-II. The different pharmacological behavior of urantide (pure antagonist in the rat aorta vs. agonist in CHOhUT cells) could be attributed to species-specific differences between rat and human UTRs. Initial pharmacological studies carried out in rats indicated that in vitro UT-II induces both endothelium-independent vasoconstriction and endothelium-dependent vasodilatation, whereas in vivo the main action of UT-II is vasodilatation [Gardiner et al., 2001].

Studies on the vascular responses to hUT-II revealed a highly variable pharmacological profile, cumulatively indicating that hUT-II is a very potent constrictor of isolated vessels from different mammalian species including human arteries and veins. The potency of UT-II as a vasoconstrictor is an order of magnitude greater than that of endothelin-1, noradrenalin, and serotonin, making UT-II the most potent mammalian vasoconstrictor identified so far [Douglas and Ohlstein, 2000]. Several in vitro studies have been conducted in human vessels, showing that the pharmacological activity of UT-II on the human vasculature differs greatly from that in other species. Moreover, UT-II causes contractions in a number of non-vascular smooth muscle tissues, such as primate airways and human heart. Taken together, these observations point out the importance of UT-II as a multifunctional peptide transmitter in mammalian systems as well as the need for further studies to definitively assess its role in human physiology and in diseases such as atherosclerosis, cardiac hypertrophy and pulmonary hypertension.

Tumor cells can produce and secrete different vasoactive peptides which act as growth stimulators in an autocrine/paracrine fashion [Asano et al., 1984; Kusuhara et al., 1990; Shichiri et al., 1991; Takahashi et al., 1998a,b, 2000; Sone et al., 2000]. UT-II mRNA has been detected in tumor cell lines of neural origin. The treatment with UT-II significantly stimulates proliferation of human adrenocortical carcinoma SW-13 and human renal cell carcinoma VMRC-RCW cell lines [Takahashi et al., 2001, 2003]. It was also reported that UT-II stimulates calcium mobilization in cells stably transfected with UTR [Camarda et al., 2004].

Prostate cancer is the most frequently diagnosed malignancy and the second leading cause of cancer-related death for men in industrialized countries. Androgen deprivation and androgen receptor (AR) blockade have been the mainstays of treatment for prostate cancer. Although initially effective, hormone therapy fails for the majority of initial responders, as subpopulations of tumor cells undergo mutations and gain capacity to proliferate in an androgen-deprived environment [Takahashi et al., 2001]. The range of severity in prostate cancer is highly variable, being from indolent to highly aggressive disease. Some patients with prostate cancer have a life expectancy similar to the general population, whereas others develop metastatic disease that can lead to death within months [Johansson et al., 1997; Halabi et al., 2003; Albertsen et al., 2005]. Clinicians have limited ability to estimate survival in patients with newly diagnosed prostate cancer, and uncertainty exists about optimal treatment decisions [Holmboe and Concato, 2000], especially for men with localized disease. Current clinical strategies [Partin et al., 1997] for evaluating prognosis in prostate cancer at the time of diagnosis include the determination of anatomical extent, histologic grade (Gleason score), and serum levels of prostate-specific antigen (PSA). The Gleason score is a widely accepted score system able to predict the aggressiveness of prostate cancer [Gleason and Mellinger, 1974].

A consensus conference for the purpose of standardizing both the perception of histologic patterns and how the grade information is compiled and reported was organized by the International Society of Urological Pathology [Egevad, 2008]. In fact, Gleason score interpretation is subjective and is left to the pathologist experience and background. Therefore, searching for homogenous criteria of evaluation is of paramount importance. Another concern linked to Gleason score evaluation is poor predictor potency in the subgroup of patients with Gleason score more or less 7 that has pushed on the finding of molecular markers predictive of response. Consequently, as a novel approach, molecular features—such as markers of cell cycle regulation and blood vessel formation—are potentially relevant prognostic factors. A recent review [Quinn et al., 2005] reported that abnormal expression of various molecular markers is related to increasing stage and grade of prostate cancer but may or may not influence long-term health outcomes. However, definite molecular markers able to predict prognosis are not known at the present.

In this study, the potential involvement of UT-II in human prostate tumorigenesis was evaluated both in vivo and in vitro. The results obtained suggest that this pathway is involved in the regulation of important phenotypic features of prostate cancer cells, such as proliferation and invasion, and that evaluation of UTR expression can provide useful prognostic information in prostate cancer patients.

MATERIALS AND METHODS

MATERIALS

RPMI 1640, DMEM, BSA, and FBS were purchased from Flow Laboratories (Milan, Italy). Tissue culture plasticware was from BectonDickinson (Lincoln Park, NJ). Rabbit antisera raised against γ-tubulin, α-tubulin, AR, focal adhesion kinase (FAK), p-FAK, Erk1/2, pERK1/2, pAkt, and GPR14 were purchased from Santa Cruz Biotechnology (Santa Cruz, CA). hUT-II and urantide, the agonist–

antagonistic compound of UT-II, were provided by Prof. P. Grieco (Department of Pharmaceutical Chemistry, University of Naples, "Federico II").

CELL CULTURE

PC3, DU145, and LNCaP prostate cancer cell lines were provided by ATCC and were grown in medium as suggested by ATCC in a humidified incubator containing 5% CO_2 at 37°C.

PROTEIN EXTRACTION AND WESTERN BLOTTING

Cell cultures were washed twice with ice-cold PBS/BSA, scraped, and centrifuged for 30 min at 4°C in 1 ml of lysis buffer (1% Triton, 0.5% sodium deoxycholate, 0.1 M NaCl, 1 mM EDTA, pH 7.5, 10 mM Na_2HPO_4, pH 7.4, 10 mM PMSF, 25 mM benzamidin, 1 mM leupeptin, 0.025 U/ml aprotinin). Equal amounts of cell proteins, monitored by Lowry assay using bovine serum albumin as standard, were separated by SDS–PAGE. The proteins on the gels were electro-transferred to nitrocellulose and reacted with the different antibodies as previously shown [Marra et al., 2009].

RNA EXTRACTION AND REAL-TIME RT-PCR

RNA was isolated from cells using Trizol (Invitrogen, Carlsbad, CA). First-strand cDNA was synthesized using 1 mg of total RNA, M-MLV Reverse Transcriptase (Sigma Chemical Co.) and random primers, as recommended by the manufacturer [Sgambato et al., 2010]. Real-time quantitative PCR (RT-PCR) analysis was carried out using a BioRad iCycler iQ Real-Time PCR System (BioRad Laboratories, Hercules, CA). Reactions were prepared in triplicate using 2× SYBR Green Supermix (BioRad Laboratories) according to manufacturer's instructions to a final volume of 25 ml. The following conditions were used: 95°C for 3 min, followed by 40 cycles at 95°C for 15 min and 60°C for 30 min. Quality of PCR products was evaluated by generating a melting curve, which was also used to verify the absence of PCR artifacts (primer–dimers) or non-specific PCR products. Results have been analyzed using the BioRad ICQ-5 software (BioRad Laboratories) and are expressed as mean UTR expression relative to mean GAPDH expression, as previously reported [Sgambato et al., 2010]. The following primer set was used for UTR: forward primer, 5'-CACGGGCACCATTGGGACTC-3'; reverse primer, 5'-CGCCAGGTTGACCACGTAGAC-3'.

INVASION AND MOTILITY ASSAYS

For motility assays, inserts (8 μm pore, Falcon) which stood in six-well plates (Costar) were employed. For in vitro invasion assays, Matrigel™ (Sigma) was diluted to 1 mg/ml in serum-free RPMI medium. One hundred microliters of 1 mg/ml Matrigel™ were placed on the lower side of each insert. The insert and the plate were incubated overnight at 4°C. The following day, cells were harvested and suspended in RPMI at a concentration of 1×10^6 cells/ml. The inserts were washed with serum-free RPMI, then 1×10^6 cells was added to each insert and 3 ml of RPMI containing 10% FCS were added to the well underneath the insert. Cells were incubated at 37°C up to 24 h. After this time, the inner side of the insert was wiped with a wet swab to remove the cells while the outer side of the insert was gently rinsed with PBS and stained with 0.25% crystal violet for 10 min, rinsed again, and then allowed to dry. The inserts were then viewed under a CCD camera equipped Nikon Optiphot microscope and quantitized as previously described [Albini et al., 1987; Colone et al., 2008].

SCANNING ELECTRON MICROSCOPY

For scanning electron microscopy (SEM) analysis, the membranes with 8.0 μm pores removed from the inserts used for the invasion and motility assays at the indicated times were fixed with 2% glutaraldehyde in 0.1 M cacodylate buffer (pH 7.4) at room temperature for 30 min, post-fixed with 1% OsO_4 in the same buffer, dehydrated through a graded ethanol series, critical point dried with CO_2, and gold coated by sputtering. Samples were examined with a Cambridge Stereoscan 360 scanning electron microscope (Cambridge Instruments Ltd, Cambridge, UK).

ANALYSIS OF ACTIVATED p-FAK

Migration assay on LNCaP prostate cancer cells was performed in presence or in absence of 1,000 nM urantide. After 24 h cells were harvested from the insert by scraper and subsequently washed twice in ice-cold Tris-buffered saline (TBS; 20 mM Tris–HCl, pH 7.6, 140 mM NaCl) and lysed at 4°C in 200 ml of lysis buffer (10 mM Tris–HCl, pH 7.6, 50 mM NaCl, 30 mM sodium pyrophosphate, 5 mM EDTA, 0.5% Nonidet P40, 1% Triton X-100, 50 mM NaF, 0.1 mM Na_3VO_4, 1 mM phenylmethylsulfonyl fluoride, and complete mini proteinase inhibitors). Cell lysates were obtained by centrifugation at 17,000 g for 30 min at 4°C. Total cell lysate (10–40 mg) was then separated on SDS–PAGE. Proteins were transferred to polyvinylidene difluoride membranes that were blocked for 1 h at room temperature with 5% BSA in TTBS. Incubations with primary anti-FAK and anti-p-FAK antibodies and with horseradish peroxidase-conjugated secondary antibody were performed in blocking solution overnight at 4°C and for 1 h at room temperature, respectively. Immunoreactive bands were visualized by the ECL kit. For loading control, membranes were incubated with monoclonal anti-α-tubulin.

MEMBRANE SURFACE DETECTION OF CD11 AND CD61

For determination of cell surface expression of CD11 and CD61, fluorescence-activated cell sorting (FACS) analysis was performed using indirect staining of CD11 and CD61. After washing with cold PBS 1×, cell pellets were incubated with specific monoclonal antibody anti-CD11, anti-CD61 (10 μg/sample), and an irrelevant IgG monoclonal antibody as a negative control for 30 min at 4°C in the dark. The cells again were washed with PBS and incubated with phycoerythrin-conjugated antimouse IgG (25 μl/sample) for 30 min at 4°C in the dark. After washing, FACS sorting was performed using a FACScan (Becton Dickinson, Mountain View, CA), and analysis was performed using CellQuest 2.0 (Becton Dickinson).

PATIENT CHARACTERISTICS AND TISSUE SAMPLES

For immunohistochemical studies, samples were obtained from a series of consecutive, unselected patients who underwent core biopsies of prostate or radical prostatectomy for prostate adeno-

carcinoma at the Policlinico of Modena (Modena, Italy) and at the NCI "Fondazione G. Pascale" of Naples (Naples, Italy) and for whom clinico-pathological data were available. After excluding cases with previous personal and/or familiar tumor history or lost to follow-up, a cohort of 195 patients with diagnosis of prostate adenocarcinoma was selected for this study with mean age at diagnosis of years 69 (range 49–85; median = 70) and a mean follow-up of months 67 (range 2–183; median = 48). In details, 55 out of 195 cases were patients not suitable to radical prostatectomy, according to current exclusion criteria, such as patients older than 72 years and/or with metastatic disease and/or high Gleason score (>7). Amongst them, 29 patients presented bone metastases at the diagnosis. Moreover, in two cases pelvic node metastases were observed contextually to radical prostatectomy.

Formalin fixed, paraffin embedded specimens were retrieved for this study from the archives of the respective Departments of Pathology and four experienced pathologists (R.F., M.M., G.B., and G.R.) confirmed the histological diagnosis of each lesion as well as the Gleason grading score. The selection did not require approval by an Institutional Review Board because the samples were coded and the names of the patients were not revealed. Follow-up information was obtained from patients' medical records and local death registries. Tumors included three Gleason score 4 (1.5%), 9 Gleason score 5 (4.6%), 38 Gleason score 6 (19.5%), 70 Gleason score 7 (35.9%), 40 Gleason score 8 (20.5%), and 35 Gleason score 9 (18.0%) carcinomas. The mean Gleason score among the 195 carcinomas was 7.2 (median 7, range 4–9). Tumor stage was determined according to the 2002 AJCC (TNM) Cancer Staging classification (Greene et al., 2002): 67 (34.3%) patients were stage II, 62 (31.8%) were stage III, and 66 were stage IV (33.9%). Hormone depleting therapy was performed in all 55 patients not suitable to radical prostatectomy and in patients who suffered disease relapse during follow-up. Radiotherapy was applied for all patients with histological positive margins of radical prostatectomy (20/195). Treatment remained reasonably consistent during the study period.

HISTOLOGY AND IMMUNOHISTOCHEMISTRY

For immunohistochemical analysis, formalin fixed, and paraffin-embedded prostate core biopsies or radical prostatectomy of patients with prostate adenocarcinoma were collected from files of Pathology Department of NCI "Fondazione G. Pascale" of Naples and from the Policlinico of Modena. Only patients with known main follow-up data have been included in our study. In details, for 100 patients we have performed UTR immunohistochemical staining of both biopsies and radical prostatectomy samples and found a good staining concordance thus suggesting that biopsy could be reasonably representative of the entire surgical sample for such a marker (data not shown). Hematoxylin–eosin slides for each one case were reviewed by expert pathologists (R.F. and G.B.), in order to confirm diagnosis, Gleason grading score and to select representative cancer areas generating Gleason grading sum. Rabbit antisera raised against GPR14 (1:3,000, Santa Cruz, CA) was used. Immunohistochemistry technique was performed as previously reported [Franco et al., 2010]. UTR expression was quantified in representative areas, previously selected, and a percentage of positive cells was recorded for both primary and secondary neoplastic areas generating Gleason grading sum. More than 30% of UTR expressing cells was recorded as high-UTR expression, whilst low expression was considered in cases with <30% of UTR expressing cells. Sections of known positive prostate carcinoma were used as positive controls. Negative controls were obtained by omitting the primary antibody.

The association between UTR expression and other molecular and clinico-pathological parameters was calculated using contingency table methods and tested for significance using the Pearson's chi-squared test. Overall survival was defined as the interval between surgery and death from the disease. Eleven patients who died for causes unrelated to disease were not included in the survival analyses. Univariate and multivariate relative risks were calculated using the Cox proportional hazards regression. All calculations were performed using the SPSS (Statistical Package for the Social Sciences rel. 13) software (Chicago, IL) and the results were considered statistically significant when the *P*-value was ≤ 0.05.

RESULTS

DETERMINATION OF UTR EXPRESSION IN PROSTATE CANCER CELLS

UTR expression was evaluated by Western blotting using a specific antibody in three different human prostate cancer cell lines (Fig. 1A). UTR was highly expressed in the LNCaP androgen-dependent prostate cancer cells, while its expression was low in PC3 and DU145 androgen-independent prostate cancer cell lines (Fig. 1A). The high expression of UTR in the LNCaP cells was

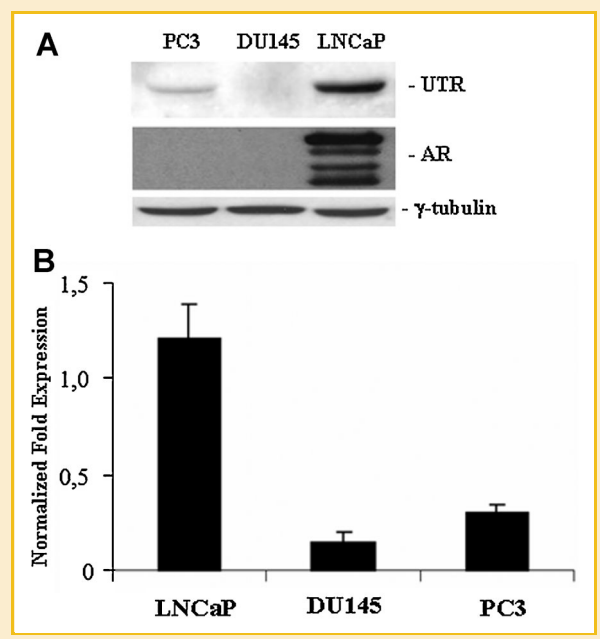

Fig. 1. UTR expression in different human cancer cell lines. A: Expression of UTR and androgen receptor (AR) in prostate cancer cells. The housekeeping protein γ-tubulin was used as loading control. B: Real-time PCR for the UTR mRNA in PC3, LNCaP, and DU145 cells (Materials and Methods Section). Bars, SDs. The experiments were performed at least three different times and the results were always similar.

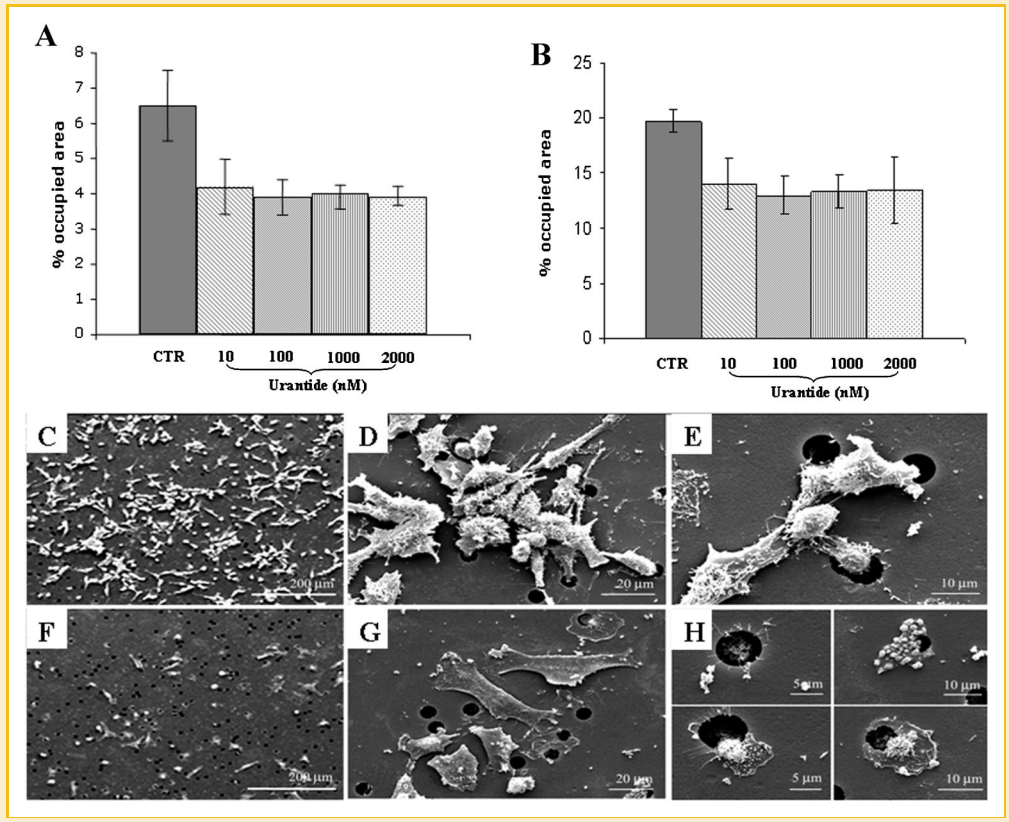

Fig. 2. Effects of the U-II antagonist urantide on motility and invasion of androgen-dependent prostate adenocarcinoma LNCaP cells. Motility and invasion assays on LNCaP cells treated with urantide, at concentrations ranging from 10 to 2,000 nM, for 48 h at 37°C migrating in the transwell chambers in the absence (A) or in the presence of Matrigel (B) as described in Materials and Methods Section. The percentage mean values of area occupied by migrated and invaded cells are reported on the ordinate. The results are the mean of three different experiments and SDs are represented as bars. SEM observations of LNCaP cell migration through 8 μm pore membranes in the transwell chamber invasion assay. The cells were treated or not with 100 nM urantide for 48 h. Lower side of the filter: untreated cells (C–E); a decrease of total cell number crossing membrane pores was observed after treatment with 100 nM Urantide (F–H).

paralleled by a high expression of AR that were, in turn, not detectable in both PC3 and DU145 cells (Fig. 1A). UTR mRNA expression was also evaluated by RT-PCR in the same cell lines and the results displayed a variable expression of the mRNA UTR. Indeed, the mRNAs for UTR in the three different cell lines revealed an about 6- and 12-fold higher expression of UTR mRNAs in LNCaP cells if compared with PC3 and DU145 cell lines, respectively (Fig. 1B).

EFFECTS OF UT-II AND URANTIDE ON PROLIFERATION, CELL MOTILITY, AND INVASION OF PROSTATE CANCER CELLS

To evaluate the effects of UTR-dependent signaling pathway on the behavior of prostate cancer cells, the biological effects of human UT-II and Urantide, a potent and competitive UT agonist–antagonist, were evaluated on the proliferation of prostate LNCaP, PC3, and DU145 cancer cell lines. Both agents displayed no significant effects on the proliferation of these three cell lines of prostate adenocarcinoma (data not shown).

In order to explore the effects on the motility and invasion processes, LNCaP cells were treated with urantide at concentrations ranging from 10 to 2,000 nM, for 30 min at 37°C. Then cells were seeded in transwell chambers and allowed to migrate and invade (membrane covered by Matrigel™) in the absence or presence of urantide. The qualitative and quantitative analysis of migration and invasion processes was carried out by SEM and computer-assisted light microscopy.

As shown in Fig. 2A,B, the treatment of the cells with urantide inhibited both cell motility and invasion reaching an about 50% maximal inhibition at 100 nM urantide. Higher urantide concentrations induced similar effects supporting the hypothesis that this agent acted as an UTR antagonist, at least in the present experimental model.

SEM analysis showed that when grown on the substrate, LNCaP cells adopted either an elongated spindle-shaped or round-shaped morphology (data not shown). During migration they moved as cluster cells, either in absence or in presence of Matrigel™ (Fig. 3). After treatment with urantide (Fig. 2F–H) an increased cell clustering was observed on the upper side of the filter (data not shown): the reinforcement of inter-cellular protrusions likely hampered cell migration through the membrane pores. On the lower side of the filter, leader cells carrying other surrounding cells were visible in control samples (Fig. 2E), while isolated and flattened cells were more frequently observed after treatment with urantide (Fig. 2H). Moreover, accordingly to quantitative analysis, a decrease of total cell number crossing membrane pores was recorded.

When the migration was performed in the presence of Matrigel™, cell clusters with leader cells were also visible on the upper side

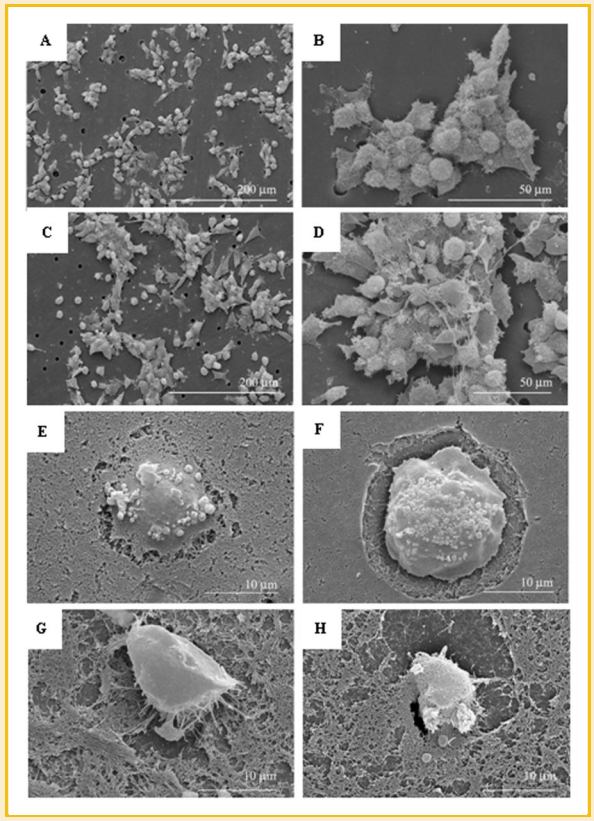

Fig. 3. Study of the morphologic changes during invasion of LNCaP cells treated or not with urantide. SEM observations of LNCaP cell invasion. When the migration was performed in the presence of Matrigel™, cell clusters with leader cells were still visible on the upper side of the filter (A,B); in agreement with results observed during migration, after the treatment with 100 nM urantide (C,D) cell clusters increased in size and fibrous material was visible on the top. To invade the Matrigel™ LNCaP cells adopt an ameboid behavior (E); images suggesting intense proteolytic degradation were observed at later phases (F). Proteolytic digestion was not inhibited by the addition of urantide, while, cell blebbing dramatically decreased (G,H).

of the filter (Fig. 3A,B). In agreement with data observed during migration, after urantide treatment (Fig. 3C,D) cell clusters increased in both size and fibrous material visible on the upper side. During the initial phase of invasion, cells infiltrated Matrigel™ through little blebbings adopting an ameboid behavior (Fig. 3E,F); however, images suggesting intense proteolytic degradation were observed at later phases (Fig. 3F,H). The treatment with urantide induced a dose-dependent reduction of invading cell number; however, images suggesting proteolytic digestion were not inhibited by the addition of urantide, while, in these experimental conditions, cell blebbing dramatically decreased (Fig. 3G,H).

EFFECTS OF URANTIDE ON ADHESION FACTORS

Integrins are heterodimeric cell surface molecules that on one side link the actin cytoskeleton to the cell membrane and on the other side mediate cell–matrix interactions. In addition to their structural functions, integrins mediate signaling from the extracellular space into the cell through integrin-associated signaling and adaptor molecules such as FAK, to regulate survival, proliferation, and cell shape as well as polarity, adhesion, migration, and differentiation. In tumor cells of diverse origin, the function and regulation of these molecules are partly disturbed and thus might contribute to the malignant phenotype and pre-existent and acquired multidrug resistance [Hehlgans et al., 2007].

FAK is a non-receptor protein tyrosine kinase that promotes both cell motility and invasion through the activation of distinct signaling pathways [Hsia et al., 2003]. FAK does not phosphorylate other substrates, but once activated it autophosphorylates and binds Src kinase which, in turn, phosphorylates FAK and FAK-binding proteins. LNCaP cells induced to migrate showed an about 30% increase of the activated form of FAK (p-FAK; Fig. 4A,B). The treatment with 100 nM urantide for 20 h induced an about 30% and 50% down-modulation of p-FAK amount in adherent and migrating cells, respectively (Fig. 4A,B). On the other hand, the treatment did not induce any change in the total FAK protein expression (Fig. 4A).

Disseminated prostate tumors are characterized by altered integrin expression. In particular, αvβ3, which is not expressed in normal prostate tissue but is upregulated in prostate adenocarcinoma, has been linked to invasive behavior [Zheng et al., 1999]. β3 integrins participate in the interaction of prostate tumor cells with extracellular matrix proteins that allow solitary cells or small groups of cells to establish metastases and, after a period of time, shift from invasive to proliferative behavior. We have evaluated the effects of urantide on both CD61 (αvβ3 integrin) and CD11 (β2 integrin) expression, both involved in cell adhesion processes (Fig. 4C–E). The treatment with 100 nM urantide for 24 h induced an about 40% reduction of the expression of both CD11a and CD61 on LNCaP cells (Fig. 4C) while milder effects were recorded on both PC3 and DU145 cell lines that express lower UTR mRNA and protein levels (Fig. 4D,E).

EFFECTS OF URANTIDE ADDITION AND UTR KNOCK-DOWN ON MOTILITY AND INVASION OF LNCAP CELLS

In order to evaluate the specific contribution of UTR in the regulation of motility and invasion of LNCaP cells, these cells were transiently transfected with a shRNA for UTR to down-regulate UTR protein expression.

Both 100 nM urantide for 48 h and transfection with shRNA for UTR produced an about 40% and 50% reduction of cell motility in Boyden chambers, respectively (Fig. 5A,C). This effect was slightly increased in transfected cells treated with urantide reaching an about 55% inhibition (Fig. 5A,C). LNCaP cells treated with urantide or transfected with shUTR cells also displayed 20% and 30% inhibition, respectively, of their ability to migrate through Matrigel matrix compared to untreated cells (Fig. 5B,C). Down-regulation of UTR in cells treated with urantide did not increase the effect induced by urantide alone (inhibition of cell invasion was about 30%; Fig. 5B,C). It is noteworthy that in transfected cells UTR expression was almost completely abrogated (Fig. 6A). These results demonstrated that UTR is involved in both motility and invasion of human androgen-dependent prostate cancer cells and its down-regulation caused by the specific shRNA induced biological effects similar to those triggered by the addition of the antagonist, even if it did not potentiate the effects of the latter.

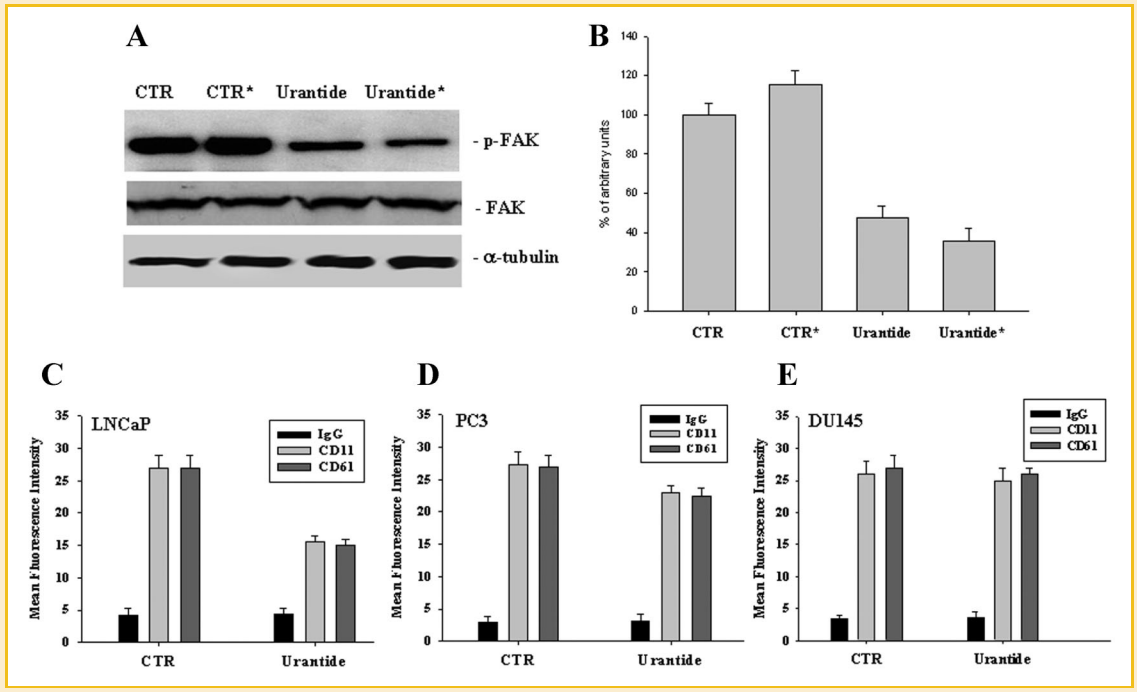

Fig. 4. Effects of urantide on adhesion factor expression on LNCaP cells. A: Determination of both total and activated form of FAK (p-FAK) evaluated after blotting with specific antibodies, as described in Materials and Methods Section. The housekeeping protein α-tubulin was used as loading control. Asterisks indicate cells induced to migrate through the addition of fetal calf serum. The experiments were performed at least three different times and the results were always similar. B: Laser scanner of the bands associated to phosphorylated isoform of FAK. The intensities of the bands were expressed as arbitrary units. Bars, SEs. Quantification, as mean fluorescence intensity, of membrane surface CD11 and CD61 expression evaluated by FACS analysis as described in Materials and Methods Section in LNCaP (C), PC3 (D), and DU145 (E) prostate cancer cell lines. CTR, untreated cells; Urantide, cells exposed to 100 nM urantide for 48 h; IgG, irrelevant monoclonal antibody. The experiments were performed at least three different times and the results were always similar.

EFFECT OF DOWN-REGULATION OF UTR ON RAS-DEPENDENT SIGNAL TRANSDUCTION PATHWAY

In order to evaluate the molecular mechanisms of the specific contribution of UTR in the regulation of motility and invasion of LNCaP cells we also evaluated the effects of UTR shRNA on proliferation and survival pathways (Fig. 6).

Down-regulation of UTR with the shRNA induced a weak increase of Erk-1/2 phosphorylation (Fig. 7A,B) and a decrease of AKT phosphorylation (Fig. 6A,B). However, both effects did not reach statistical significance (Fig. 6B).

Moreover, we investigated the effects of both urantide and shRNA for UTR on the expression and activation of proteins belonging to Ras family such as RhoA and RhoC that are both involved in the regulation of cell adhesion and invasion. RhoA and RhoC activation ratios were calculated as the ratio between the intensities of the bands associated with either RhoA or RhoC activity and expression, respectively. RhoC activity and function were both increased by UTR down-modulation induced by either shRNA transfection or urantide (Fig. 6C). Therefore, the RhoC activation ratio was not modified by both UTR knock down and by the addition of the UT-II antagonist urantide (Fig. 6D). On the other hand, both down-regulation of UTR and urantide addition caused a decrease of RhoA expression without changing RhoA function (Fig. 6C). Therefore, either urantide addition or down-regulation of UTR increased RhoA activation ratio (Fig. 6D) suggesting relevant effects of UTR on the activity of RhoA.

UTR EXPRESSION IS REDUCED IN HUMAN PRIMARY PROSTATE CANCERS AND CORRELATES WITH THE CLINICAL OUTCOME OF PATIENTS

In order to investigate UTR changes occurring in human prostate tumorigenesis, UTR expression was evaluated by immunostaining in a series of 195 human prostate tissue samples collected from patients who underwent core biopsy or radical prostatectomy for prostate adenocarcinoma and the results were correlated with other available clinical–pathological parameters.

UTR was slightly expressed in benign prostate hyperplasia near neoplastic area whilst variable expression was observed in cancer cells with an intensity inversely correlated to the grading score (Fig. 7A–E). In Figure 7F, it is shown a lymph node metastasis expressing low-UTR levels.

In tumors ($n = 195$) the median percentage of positive cells was 30 (range 0–90; mean = 32) and UTR staining was not detectable in tumor cells in 19 (10%) specimens. When tumors were stratified according with tumor grade, mean percentage of positive cells was 46 (range 5–90), 34 (range 0–90), and 21 (range 0–90) in low (Gleason score ≤ 6), medium, and high (>7) grade tumors, respectively, and these differences were statistically significant. Similarly, mean percentage of positive cells was 36 (range 0–80), 31 (range 0–90), and 29 (range 0–80) in II, III, and IV stage tumors, respectively, but these differences were not significant.

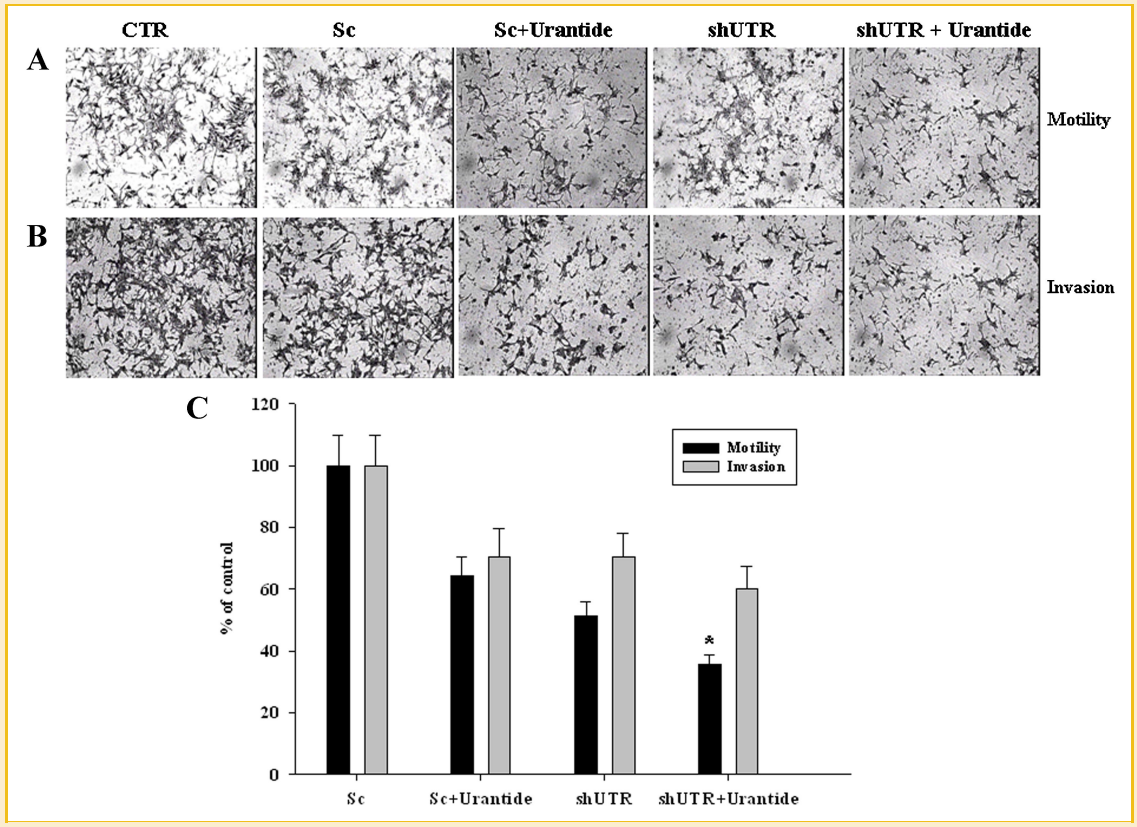

Fig. 5. Effect of down-regulation or block of UTR with either an anti-UTR shRNA or the specific antagonist urantide on cell motility and invasion of LNCaP cells. A: LNCaP parental (CTR) or transiently transfected with a shRNA for UTR (shUTR), were plated in the top chamber of non-coated polyethylene teraphthalate (PET) membranes, treated or not with 100 nM urantide for 48 h and cell motility was evaluated as described in Materials and Methods Section. B: For in vitro invasion assays, LNCaP cells were added to a Boyden chamber coated with Matrigel and cell invasion was evaluated as described in Materials and Methods Section. The migrating and the invading cells were stained with 0.25% crystal violet for 10 min and photographed under a microscope. C: The histogram shows the quantification of the migrating and invading cells measured with a spectrophotometer as OD, and the results are expressed as a percentage as compared to untreated LNCaP parental cells. The experiments were performed three different times and the results are the mean of the obtained values. Bars, SDs. CTR, untreated LNCaP cells; Sc, LNCaP cells transfected with scrambled vector and cultured for 48 h; Sc + UR, LNCaP cells transfected with scrambled vector and exposed for 48 h to 100 nM urantide; shUTR, LNCaP cells transfected with shUTR and cultured for 48 h; shUTR + UR, LNCaP cells transfected with shUTR and exposed to 100 nM urantide for 48 h. Asterisks indicate the statistical significance of the data ($P < 0.005$).

Using the 30% positive cells as cut-off to distinguish between high (>30%) and low (≤30%) UTR staining and stratifying tumors in low (Gleason score <7), medium (7), and high (>7) grade according with Gleason score, high-UTR staining was detected in 34 (68%) of the 50 low grade, 36 (52%) of the 70 medium, and in 19 (25%) of the 75 high-grade tumors, and these differences were highly significant ($P = 0.001$; Table I). Similarly, high-UTR staining decreased with increasing tumor stage being detectable in 57%, 42%, and 38% of II, III, and IV stage tumors, respectively, but these differences were not significant ($P = 0.07$; Table I).

Follow-up data were available for 184 patients including 83 (45%) high and 101 (55%) low-UTR expressing tumors. Twenty-one (25%) of the 83 high-UTR expressing and 47 (47%) of the 101 low-UTR expressing patients died of the disease during the period of follow-up and the Kaplan–Meier curves displayed a significant separation between the two groups of tumors ($P = 0.001$ by log-rank test; Fig. 8A).

UTR staining displayed a significant association with Gleason score, which is an important prognostic factor for prostate cancer patients (Table I). Thus, the negative prognostic significance of low-UTR staining could be simply a consequence of its association with higher Gleason score. To exclude this possibility, we aimed to evaluate the prognostic significance of UTR staining within a more homogeneous group of patients. When only patients with high-grade (Gleason score >7) tumors were analyzed separately (n = 70), 34 (63%) of the 54 patients with low-UTR expressing tumors, and 2 (13%) of the 16 remaining cases died during the period of follow-up. In fact, the Kaplan–Meier curves of disease-free survival displayed a significant separation between the two groups of patients ($P = 0.001$ by log-rank test; Fig. 8B). A similar result was also obtained by combining medium (Gleason score = 7) and high-grade tumors (Gleason score >7; n = 136). Forty-two (49%) of the 85 patients with low-UTR expressing tumors and only 12 (23%) of the 51 remaining cases died of disease during the period of follow-up and the Kaplan–Meier curves of overall survival displayed a significant separation ($P = 0.001$; Fig. 8C). On the other hand, we have evaluated the correlations between UTR expression and PSA levels in patients with prostate cancer and we have not found any statistically significant association between this two prognostic factors (data not shown).

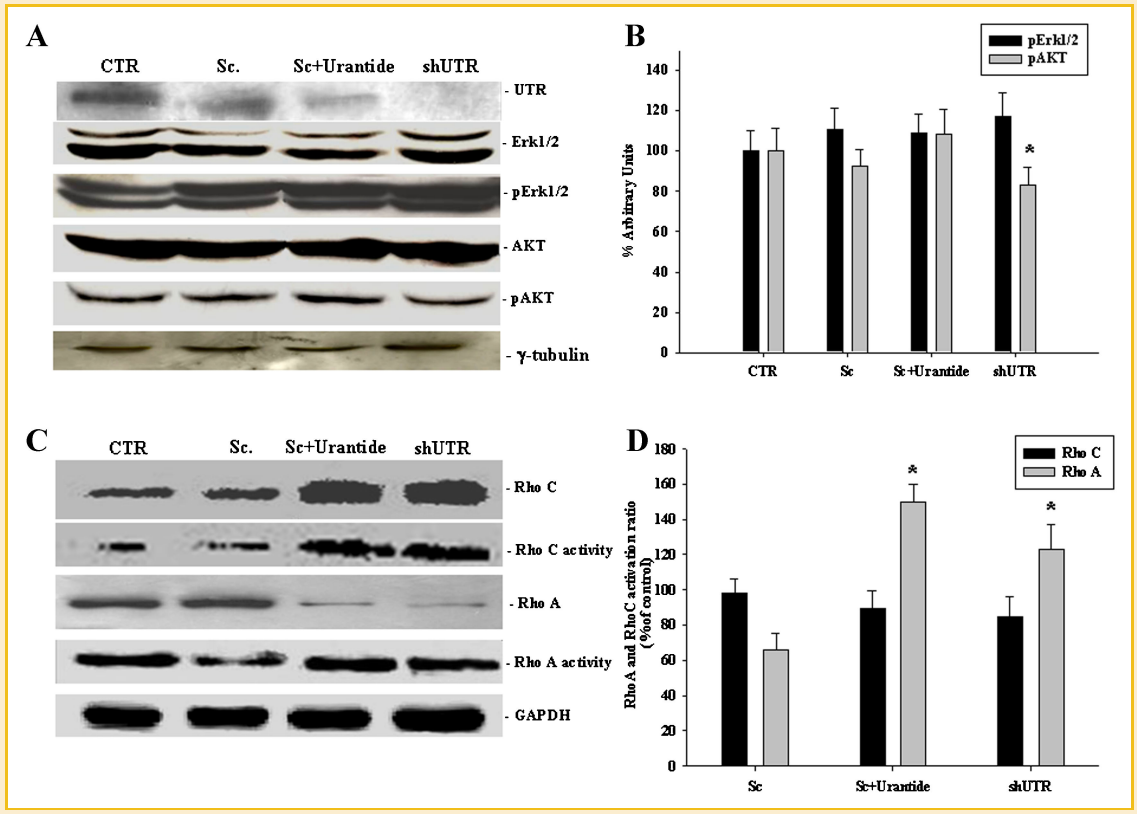

Fig. 6. Effect of down-regulation or block of UTR with either an anti-UTR shRNA or the specific antagonist urantide on signal transduction pathways. A: Western blot assay for the expression of the total UTR, Erk1/2, and Akt proteins and determination of the phosphorylation of Erk-1/2 and Akt evaluated after blotting with an anti-pMAPK and anti-pAkt specific antibody, respectively, as described in Material and Methods Section. The housekeeping protein γ-tubulin was used as loading control. B: Laser scanner of the bands associated to Erk and Akt activity. The intensities of the bands were expressed as % arbitrary units. Bars, SEs. C: Western blot assay for the expression of the total RhoA and RhoC proteins and affinity precipitation of RhoA and RhoC performed with the Rhotekin Rho binding domain, conjugated with agarose for the evaluation of RhoA and RhoC activity as described in Materials and Methods Section. The housekeeping protein GAPDH was used as loading control. D: Representation of the RhoA and RhoC activation ratio expressed as the ratio between the relative intensities of the bands associated with activated RhoA and RhoC versus the bands associated with total RhoA and RhoC, respectively. The evaluation was performed with the dedicated software after laser scanner and computer-assisted acquisition of the bands. The intensity of each band was calculated in relative intensity when compared to that of the untreated cells. The experiments were performed at least three different times and the results were always similar. CTR, untreated LNCaP cells; Sc, LNCaP cells transfected with scrambled vector and cultured for 48 h; Sc + UR, LNCaP cells transfected with scrambled vector and exposed for 48 h to 100 nM urantide; shUTR, LNCaP cells transfected with shUTR and cultured for 48 h; shUTR + UR, LNCaP cells transfected with shUTR and exposed to 100 nM urantide for 48 h. Asterisks indicate the statistical significance of the data ($P < 0.005$).

High-tumor stage ($P = 0.001$) and high-Gleason score ($P = 0.009$) were also associated with a shorter overall survival (data not shown). In a multivariate analysis performed by building a Cox hazards model that included age, Gleason score, tumor stage, and UTR staining, only a low-UTR staining ($P = 0.003$; CI = 1.323–3.828; RR = 2.25) and a high-tumor stage ($P = 0.001$; CI = 1.712–6.347; RR = 3.3) confirmed to be independent predictors of shorter survival in our series of prostate cancer patients (Table II).

DISCUSSION

To our knowledge this is the first study analyzing the expression levels of UTR in human primary prostate cancers and prostate cancer cell lines. UTR was easily detected in the androgen-dependent LNCaP cells while its expression was strikingly reduced in the androgen-independent PC3 and DU145 prostate cancer cells. Our results suggest a complex regulation of UTR expression likely also involving post-translational mechanisms since protein expression levels did not strictly correlated with mRNA expression levels. We also analyzed UTR expression in vivo on prostate tissue samples. Although UTR expression was already reported in cancer cell lines in vitro its expression has never been evaluated, at least to our knowledge, on cancer tissues in vivo [Takahashi et al., 2001, 2003]. In primary human prostate cancers UTR expression was lost in 10% of tumors and a reduced expression (≤30% positive cells) of the protein was significantly associated with higher Gleason score ($P = 0.001$), but not with other clinical-pathological features. Survival analyses by Kaplan–Meier demonstrated that in univariate analysis, reduced UTR expression was associated with an increased risk of death for disease.

UTR represents a potentially useful prognostic marker for prostate cancer patients. In fact, its expression correlated to other known pathological indicators of aggressive cancers, such as Gleason score.

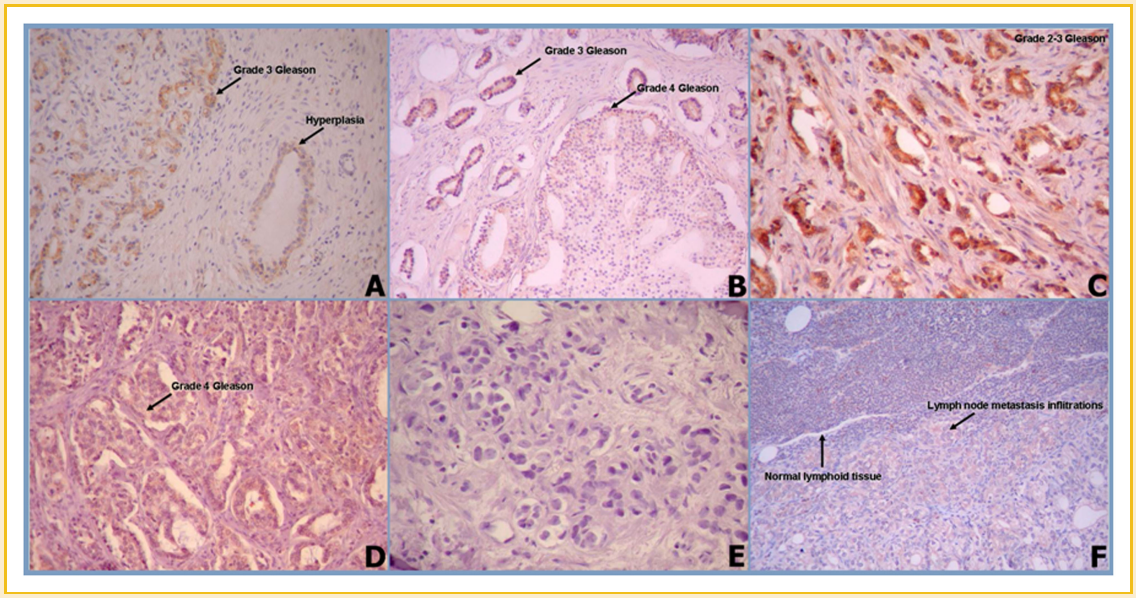

Fig. 7. Expression of UTR in human prostate tissue samples. Brown immunohistochemical staining identifies UTR positivity. A: 20×, arrows indicate UTR-positive staining of a well-differentiated adenocarcinoma (Gleason 3 area) and slight and focal positivity of normal prostatic ducts. B: 20×, arrows indicate high-UTR-positive staining of a Gleason 3 area compared to a focal positivity in a Gleason 4 area. C: 40×, high-UTR positivity in a Gleason 3 area. D: 40×, focal and slight UTR-positive staining in a Gleason 4 area. E: 40×, absence of UTR expression in a Gleason 5 area. F: 20×, focal UTR-positive staining in a prostatic adenocarcinoma nodal metastasis.

It is noteworthy that reduced UTR expression confirmed to be a negative prognostic indicator of poor survival in the subset of patients with medium and/or high (Gleason score $\geq$7) grade tumors. These data support the significance of UTR expression as a prognostic marker in prostate cancer patients. Another interesting consideration is that reduced UTR expression confirmed to be an independent prognostic indicator when analyzed in a multivariate model also including Gleason score and tumor stage. A clinical implication of these findings is to establish the prognostic score of patients affected by prostate cancer independently from Gleason score. The definition of the prognosis in these patients is an important and debated issue. In fact, part of these patients continues to have a long-lasting androgen-responsive disease while another group rapidly develops an aggressive and hormone-refractory cancer. Thus, the early definition of the clinical outcome of these patients has important consequences on the choice of the optimal personalized therapeutic and follow-up strategy. Therefore, the research of molecular markers that can be valid alternative and/or additional tools to Gleason score has been widely exploited in the last years [Quinn et al., 2005] but until now no definitive results have been achieved. We believe our findings are of interest and additional studies on the potential prognostic significance of UTR in prostate cancer patients are warranted since tumor tissue is routinely available for immunostaining that is a routinely performed, simple, inexpensive, and reliable assay.

TABLE I. UTR Expression in Relation to Clinical and Pathological Parameters in a Series of 195 Prostate Cancer Patients

	Total	Low, n (%)	High, n (%)	
	195	106 (54)	89 (46)	*P*-value
Age (years)				
≤70	109	62 (57)	47 (43)	0.04
>70	86	44 (51)	42 (49)	
Tumor stage				
II	67	29 (43)	38 (57)	0.07
III	62	36 (58)	26 (42)	
IV	66	41 (62)	25 (38)	
Gleason score				
Low	50	16 (32)	34 (68)	0.001
Medium	70	34 (49)		
High	75	56 (75)	19 (25)	

To additionally investigate upon the role of UTR in prostate epithelial cells we also studied the biological functions of UTR on in vitro prostate cancer cells using either the UT-II antagonist urantide or a shRNA for UTR able to down-regulate UTR expression in LNCaP cells. The well-known effects of UT-II/UTR network on the intracellular Ca^{++} release and smooth muscle cell contraction [Douglas and Ohlstein, 2000; Gardiner et al., 2001; Takahashi et al., 2001, 2003; Camarda et al., 2004] encouraged us to study the effects of urantide and shRNA-mediated UTR knock-down on both LNCaP cell motility and invasion. Surprisingly, we found that the down-regulation of either the function and/or expression of UTR have significant effects on the motility and, at a lesser extent, on invasion of prostate cancer cells. These effects were paralleled by both decreased CD61 and CD11a integrin expression and FAK tyrosine phosphorylation. FAK is a target of integrins and promotes cell motility and invasion through the activation of distinct signaling pathways [Hsia et al., 2003]. Several reports connect FAK to cell migration and invasion. FAK is a non-receptor protein tyrosine kinase involved in signal transduction from integrin-enriched focal adhesion sites that mediate cell contact with the extracellular

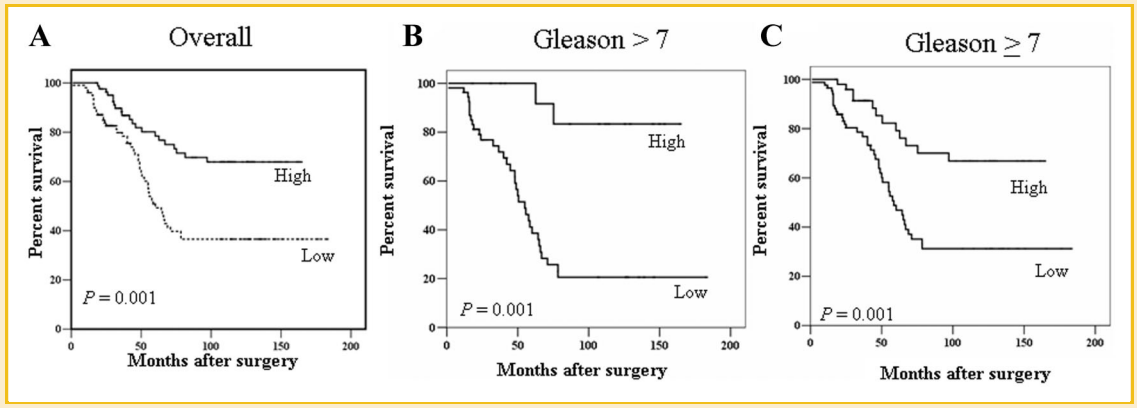

Fig. 8. Kaplan–Meier curves for overall survival in a series of 184 prostate cancer patients. Curves represent overall survival of patients stratified by UTR expression. A: All patient population was included in the analysis. B: Only patients (n = 70) with high-grade (Gleason score >7) tumors were included in the analysis. C: Patients (n = 136) with both medium (Gleason score = 7) and high-grade (Gleason score >7) tumors were included in the analysis.

matrix. Multiple protein–protein interaction sites allow FAK to associate with adapter and structural proteins allowing the modulation of mitogen-activated protein (MAP), stress-activated protein (SAP) kinases, and small GTPase activity. The enhancement of FAK-mediated signaling has been shown to mediate the survival of anchorage-dependent cells and are critical for efficient cell migration in response to growth factor receptor and integrin stimulation. Elevated expression of FAK in human tumors has been correlated with increased malignancy and invasion. As recent findings show that FAK contributes to the secretion of matrix-metalloproteinases, FAK represents an important checkpoint in coordinating the dynamic processes of cell motility and extracellular matrix remodeling during tumor cell invasion [Hauck et al., 2002]. Additional uncharacterized connections between FAK and Rho GTPases also exist, as FAK-deficient cells exhibit elevated RhoA that is repressed upon FAK re-expression [Ren et al., 2000]. As the FAK-associated Rho-GAP protein Graf could represent a negative regulator of Rho GTPases, it is possible that FAK may modulate Rho activity via the recruitment and activation of Graf [Taylor et al., 1999]. It is likely that activation of Rac and Cdc42 activity coupled with the inhibition of RhoA by FAK is an important cross-talk promoting the dynamic regulation of the actin cytoskeleton.

TABLE II. Contribution of Various Potential Prognostic Factors to Overall Survival by Cox Regression Analysis in Prostate Cancer Patients

Variable	Risk ratio	95% Confidence interval	*P*-value
Age[a]	1.412	0.876–2.276	0.109027778
Gleason score[b]	1.012	0.547–1.907	0.658333333
Tumor stage[c]	3.296	1.712–6.347	0.001
UTR[d]	2.250	1.323–3.828	0.003

[a]The risk ratio is given as older versus younger patients (cut-off = 70 years).
[b]The risk ratio is given as higher (>7) versus lower Gleason score.
[c]The risk ratio is given as higher (stage IV) versus lower stage cancers.
[d]The risk ratio is given as low (≤30% positive cells) versus high (>30%) expressor tumors.

The role of Rho for cell migration is supported by a recent imaging study analyzing the localization of active Rho in migrating fibroblasts [Pertz et al., 2006]. The involvement of RhoA in the regulation of migration is complex and is likely related to alternate processes of activation and inactivation. In our experimental conditions, we have found that inhibition of LNCaP cell migration induced by urantide was paralleled by the decreased phosphorylation of FAK and increased activity of RhoA [Narumiya et al., 2009]. On the other hand, RhoC was verified as a potential metastasis gene by expressing exogenous RhoC in melanoma cells and examining lung metastases. The selected metastatic cell population and the cells over-expressing exogenous RhoC did not show enhanced proliferation, but were more migratory and more invasive and exhibited elongated morphology. These properties are suppressed by expressing dominant negative Rho mutants. More recently, analysis of microRNAs (miRNAs) expressed in breast cancer also identified RhoC as a metastasis-associated gene [Clark et al., 2000]. In our experimental model, we have found a slighter decrease of cell invasion of cells treated by urantide that was not paralleled by significant changes in RhoC acitivity thus confirming poor involvement of UTR in the regulation of invasive processes.

During the initial phase of invasion, cells infiltrate the Matrigel™ film by little blebs in the absence of proteolytic degradation, by adopting an ameboid behavior. The ameboid motility does not require extracellular proteases [Wolf et al., 2003] but is associated with the formation of small, bleb-like protrusions being dependent upon ROCK activity. Apparently, LNCaP cells constitutively use the mesenchymal mode of invasion. Mesenchimal mode of invasion is coupled to the cleavage and remodeling of ECM components using metalloproteases (MMPs) and other proteases [Ishibashi et al., 1999; Bachmeier et al., 2001]. It has been shown that MMPs are secreted by the human prostate gland, both in vivo and in vitro, and higher expression levels of MMP-2 are associated with increasing Gleason score, tumor metastasis, and aggressive behavior of prostate cancer [Lokeshwar, 1999]. Moreover, we have recently reported that prostate cancer patients responsive to treatment have a significant decrease of circulating MMPs [Facchini et al., 2010]. In our experimental model prostate tumor cells recurred to an

ameboid movement during the initial phase of migration process; thereafter, proteolytic mesenchimal digestion did occur, indicating that contractile force generation triggered by Rho/ROCK signaling was induced in the early phase of the cell receptor interaction with extracellular matrix. The treatment with urantide or anti-UTR shRNA induced a dose-dependent reduction of migrating and, at a less extent, invading cell number: proteolytic digestion was not hampered, but both cell blebbing and migration dramatically decreased, accordingly to the increase of Rho A activity induced by the treatment.

The expression of UTR in the initial Gleason score found in our series supports the role of this receptor in the initial stages of prostate cancer tumorigenesis in which cell movements are important in order to determine the initial invasion of the surrounding parenchyma and the formation of convoluted glands. In the advanced Gleason score, the digestion of the parenchyma by proteases becomes essential for the progression of the cancer that begins to display other phenotypic changes relevant for the spreading in distant organs (lymph nodes and bone). Moreover, the in vitro data suggesting that the function and expression of UTR were closely associated with prostate cancer cell invasion and migration are in agreement with UTR staining which showed a trend of decreasing values with increasing tumor stage ($P = 0.07$). The lack of significance is likely to be attributed to the complex regulation of such phenomenon in vivo. However, the in vivo data further support the role of UTR-dependent pathways in cancer progression in vivo and warrant further studies on this subject that is not the focus of the present manuscript.

In conclusion, we have found a new molecular marker that can be used together with Gleason score in the diagnostic and prognostic definition of prostate cancer patients able to discriminate the patients with good prognosis even within subsets with same Gleason score. Moreover, we have studied the biological role of UTR in prostate adenocarcinoma and obtained data suggesting its involvement in the regulation of cell motility. Overall, these data suggest that UTR can be considered a prognostic marker in human prostate adenocarcinoma patients.

ACKNOWLEDGMENTS

This study was partially supported by Italian Ministry of Health FSN 2007-Progetto Strategico Oncologia. M.C. received a grant by Regione Campania Laboratori Pubblici "Hauteville."

REFERENCES

Albertsen PC, Hanley JA, Fine J. 2005. 20-Year outcomes following conservative management of clinically localized prostate cancer. JAMA 293:2095–2101.

Albini A, Iwamoto Y, Kleinman HK, Martin GR, Aaronson SA, Kozlowski JM, McEwan RN. 1987. A rapid in vitro assay for quantitating the invasive potential of tumor cells. Cancer Res 47:3239–3245.

Ames RS, Sarau HM, Chambers JK, Willette RN, Aiyar NV, Romanic AM, Louden CS, Foley JJ, Sauermelch CF, Coatney RW, Ao Z, Disa J, Holmes SD, Stadel JM, Martin JD, Liu WS, Glover GI, Wilson S, McNulty DE, Ellis CE, Elshourbagy NA, Shabon U, Trill JJ, Hay DW, Ohlstein EH, Bergsma DJ, Douglas SA. 1999. Human urotensin-II is a potent vasoconstrictor and agonist for the orphan receptor GPR14. Nature 401:282–286.

Asano T, Aoyagi M, Hirakawa K, Ikawa Y. 1984. Effect of endothelin-1 as growth factor on a human glioma cell line, its characteristic promotion of DNA synthesis. J Neurooncol 18:1–7.

Bachmeier BE, Nerlich AG, Lichtinghagen R, Sommerhoff CP. 2001. Matrix metalloproteinases (MMPs) in breast cancer cell lines of different tumorigenicity. Anticancer Res 21:3821–3828.

Camarda V, Song W, Marzolac E, Spagnol M, Guerrini R, Salvadori S, Regoli D, Thompson JP, Rowbotham DJ, Behm DJ, Douglas SA, Calo' G, Lambert DG. 2004. Urantide mimics urotensin-II induced calcium release in cells expressing recombinant UT receptors. Eur J Pharmacol 498:83–86.

Carotenuto A, Grieco P, Novellino E, Rovero P. 2004. Urotensin-II receptor peptide agonists. Med Res Rev 24:577–588.

Clark EA, Golub TR, Lander ES, Hynes RO. 2000. Genomic analysis of metastasis reveals an essential role for RhoC. Nature 406:532–535.

Colone M, Calcabrini A, Toccacieli L, Bozzuto G, Stringaro A, Gentile M, Cianfriglia M, Ciervo A, Caraglia M, Budillon A, Meo G, Arancia G, Molinari A. 2008. The multidrug transporter P-glycoprotein. A mediator of melanoma invasion? J Invest Dermatol 128:957–971.

Douglas SA, Ohlstein EH. 2000. Human urotensin II the most potent mammalian vasoconstrictor identified to date as a therapeutic target for the management of cardiovascular disease. Trends Cardiovasc Med 10:229–237.

Egevad L. 2008. Recent trends in Gleason grading of prostate cancer II prognosis reproducibility and reporting. Anal Quant Cytol Histol 30:254–260.

Facchini G, Caraglia M, Morabito A, Marra M, Piccirillo MC, Bochicchio AM, Striano S, Marra L, Nasti G, Ferrari E, Leopardo D, Vitale G, Gentilini D, Tortoriello A, Catalano A, Budillon A, Perrone F, Iaffaioli RV. 2010. Metronomic administration of zoledronic acid and taxotere combination in castration resistant prostate cancer patients: Phase I ZANTE trial. Cancer Biol Ther [Epub ahead of print].

Franco R, Cantile M, Scala S, Catalano E, Cerrone M, Scognamiglio G, Pinto A, Chiofalo MG, Caracò C, Anniciello AM, Abbruzzese A, Caraglia M, Botti G. 2010. Histomorphologic parameters and CXCR4 mRNA and protein expression in sentinel node melanoma metastasis are correlated to clinical outcome. Cancer Biol Ther 9:423–429.

Gardiner SM, March JE, Kemp PA, Bennett T. 2001. Depressor and regionally-selective vasodilator effects of human and rat urotensin II conscious rats. Br J Pharmacol 132:1625–1629.

Gleason DF, Mellinger GT. 1974. Prediction of prognosis for prostatic adenocarcinoma by combined histological grading and clinical staging. J Urol 11:58–64.

Greene F, Page D, Fleming I, Fritz A, Bach C, Haller D, Morrow M. 2002. American Joint Committee on Cancer Staging Manual (6th ed.) Springer, New York.

Halabi S, Small EJ, Kantoff PW, Kattan MW, Kaplan EB, Dawson NA, Levine EG, Blumenstein BA, Vogelzang NJ. 2003. Prognostic model for predicting survival in men with hormone-refractory metastatic prostate cancer. J Clin Oncol 21:1232–1237.

Hauck CR, Hsia DA, Schlaepfer DD. 2002. The focal adhesion kinase—A regulator of cell migration and invasion. IUBMB Life 53:2115–2119.

Hehlgans S, Haase M, Cordes N. 2007. Signalling via integrins: Implications for cell survival and anticancer strategies. Biochim Biophys Acta 1775:163–180.

Holmboe ES, Concato J. 2000. Treatment decisions for localized prostate cancer, asking men what's important. J Gen Intern Med 15:694–701.

Hsia DA, Mitra SK, Hauck CR, Streblow DN, Nelson JA, Ilic D, Huang S, Li E, Nemerow GR, Leng J, Spencer KS, Cheresh DA, Schlaepfer DD. 2003. Differential regulation of cell motility and invasion by FAK. J Cell Biol 160:753–767.

Ishibashi O, Mori Y, Kurokawa T, Kumegawa M. 1999. Breast cancer cells express cathepsins B and L but not cathepsins K or H. Cancer Biochem Biophys 17:69–78.

Johansson JE, Holmberg L, Johansson S, Bergström R, Adami HO. 1997. Fifteen year survival in prostate cancer: A prospective population-based study in Sweden. JAMA 277:467–471.

Kusuhara M, Yamaguchi K, Nagasaki K, Hayashi C, Suzaki A, Hori S, Handa S, Nakamura Y, Abe K. 1990. Production of endothelin in human cancer cell lines. Cancer Res 50:3257–3261.

Lavecchia A, Cosconati S, Novellino E. 2005. Architecture of the human urotensin II receptor, comparison of the binding domains of peptide and non-peptide urotensin II agonists. J Med Chem 48:2480–2492.

Lokeshwar BL. 1999. MMP inhibition in prostate cancer. Ann NY Acad Sci 878:271–289.

Marra M, Santini D, Meo G, Vincenzi B, Zappavigna S, Baldi A, Rosolowski M, Tonini G, Loeffler M, Lupu R, Addeo SR, Abbruzzese A, Budillon A, Caraglia M. 2009. Cyr61 downmodulation potentiates the anticancer effects of zoledronic acid in androgen-independent prostate cancer cells. Int J Cancer 125:2004–2013.

Narumiya S, Tanji M, Ishizaki T. 2009. Rho signaling ROCK and mDia1 in transformation metastasis and invasion. Cancer Metastasis Rev 28:65–76.

Partin AW, Kattan MW, Subong EN, Walsh PC, Wojno KJ, Oesterling JE, Scardino PT, Pearson JD. 1997. Combination of prostate-specific antigen clinical stage and Gleason score to predict pathological stage of localized prostate cancer: A multi-institutional update. JAMA 277:1445–1451.

Patacchini R, Santicioli P, Giuliani S, Grieco P, Novellino E, Rovero P, Maggi CA. 2003. Urantide, an ultrapotent urotensin II antagonist peptide in the rat aorta. Br J Pharmacol 140:1155–1158.

Pertz O, Hodgson L, Klemke RL, Hahn KM. 2006. Spatio-temporal dynamics of RhoA activity in migrating cells. Nature 440:1069–1072.

Quinn DI, Henshall SM, Sutherland RL. 2005. Molecular markers of prostate cancer outcome. Eur J Cancer 41:858–887.

Ren X, Kiosses WB, Sieg DJ, Otey CA, Schlaepfer DD, Schwartz MA. 2000. Focal adhesion kinase suppresses Rho activity to promote focal adhesion turnover. J Cell Sci 113:3673–3678.

Sgambato A, Puglisi MA, Errico F, Rafanelli F, Boninsegna A, Rettino A, Genovese G, Coco C, Gasbarrini A, Cittadini A. 2010. Post-translational modulation of CD133 expression during sodium butyrate-induced differentiation of HT29 human colon cancer cells: Implications for its detection. J Cell Physiol 224:234–241.

Shichiri M, Hirata Y, Nakajima T, Ando K, Imai T, Yanagisawa M, Masaki T, Marumo F. 1991. Endothelin-1 is an autocrine/paracrine growth factor for human cancer cell lines. J Clin Invest 87:1867–1871.

Sone M, Takahashi K, Totsune K, Murakami O, Arihara Z, Satoh F, Mouri T, Shibahara S. 2000. Expression of endothelin-1 and endothelin receptors in cultured human glioblastoma cells. J Cardiovasc Pharmacol 26:S390–S392.

Takahashi K, Hara E, Murakami O, Totsune K, Sone M, Satoh F, Kumabe T, Tominaga T, Kayama T, Yoshimoto T, Shibahara S. 1998a. Production and secretion of endothelin-1 by cultured choroid plexus carcinoma cells. J Cardiovasc Pharmacol 31:S367–S369.

Takahashi K, Nakayama M, Shibahara S. 1998b. Production and secretion of neuropeptides by nervous system tumors. Cancer J 11:237–241.

Takahashi K, Yoshinoya A, Murakami O, Totsune K, Shibahara S. 2000. Production and secretion of two vasoactive peptides adrenomedullin and endothelin-1 by cultured human adrenocortical carcinoma cells. Peptides 21:251–256.

Takahashi K, Totsune K, Murakami O, Shibahara S. 2001. Expression of urotensin II and urotensin II receptor mRNAs in various human tumor cell lines and secretion of urotensin II-like immunoreactivity by SW-13 adrenocortical carcinoma cells. Peptides 22:1175–1179.

Takahashi K, Totsune K, Murakami O, Arihara Z, Noshiro T, Hayashi Y, Shibahara S. 2003. Expression of urotensin II and its receptor in adrenal tumors and stimulation of proliferation of cultured tumor cells by urotensin II. Peptides 24:301–306.

Taylor JM, Macklem MM, Parsons JT. 1999. Cytoskeletal changes induced by GRAF the GTPase regular associated with focal adhesion kinase are mediated by Rho. J Cell Sci 112:231–242.

Wolf K, Mazo I, Leung H, Engelke K, von Andrian UH, Deryugina EI, Strongin AY, Bröcker EB, Friedl P. 2003. Compensation mechanism in tumor cell migration: Mesenchymal–amoeboid transition after blocking of pericellular proteolysis. J Cell Biol 160:267–277.

Zheng DQ, Woodward AS, Fornaro M, Tallini G, Languino LR. 1999. Prostatic carcinoma cell migration via $\alpha_V\beta_3$ integrin is modulated by a focal adhesion kinase pathway. Cancer Res 59:1655–1664.